Systems/Circuits

Large-Scale Axonal Reorganization of Inhibitory Neurons following Retinal Lesions

Sally A. Marik, Homare Yamahachi, Stephan Meyer zum Alten Borgloh, and Charles D. Gilbert
Laboratory of Neurobiology, The Rockefeller University, New York, New York 10065

The functional properties of adult cortical neurons are subject to alterations in sensory experience. Retinal lesions lead to remapping of cortical topography in the region of primary visual cortex representing the lesioned part of the retina, the lesion projection zone (LPZ), with receptive fields shifting to the intact parts of the retina. Neurons within the LPZ receive strengthened input from the surrounding region by growth of the plexus of excitatory long-range horizontal connections. Here, by combining cell type-specific labeling with a genetically engineered recombinant adeno-associated virus and *in vivo* two-photon microscopy in adult macaques, we showed that the remapping was also associated with alterations in the axonal arbors of inhibitory neurons, which underwent a parallel process of pruning and growth. The axons of inhibitory neurons located within the LPZ extended across the LPZ border, suggesting a mechanism by which new excitatory input arising from the peri-LPZ is balanced by reciprocal inhibition arising from the LPZ.

Introduction

The adult brain adapts to experiences throughout life, and its plasticity extends to primary sensory cortical areas. This is seen most dramatically in the remapping of cortical topography following sensory loss. In the primary visual cortex (V1) following retinal lesions, the lesion projection zone (LPZ) is initially silenced and rendered unresponsive to visual stimuli. Soon after making the lesion, the receptive fields (RFs) of neurons located just within the LPZ border are enlarged and shifted outside the retinal scotoma. In the following months, more central locations within the LPZ recover visually driven activity with even larger shifts in RF position (Gilbert et al., 1990; Kaas et al., 1990; Heinen and Skavenski, 1991; Gilbert and Wiesel, 1992; Chino et al., 1995; Das and Gilbert, 1995a, b; Calford et al., 2000; Giannikopoulos and Eysel, 2006; Palagina et al., 2009). These changes are rapid, extensive, long-lasting and ubiquitous across sensory maps (Merzenich et al., 1983a,b, 1984; Simons and Land, 1987; Sanes et al., 1988, 1990; Robertson and Irvine, 1989; Cusick et al., 1990; Gilbert et al., 1990; Kaas et al., 1990; Heinen and Skavenski, 1991; Pons et al., 1991; Gilbert and Wiesel, 1992; Chino et al., 1995; Das and Gilbert, 1995a; Nudo et al., 1996; Schmid et al., 1996; Wallace and Fox, 1999; Calford et al., 2000).

Because of the topographic nature of the cortical reorganization following retinal lesions, V1 has proven to be an ideal model for elucidating the underlying circuit mechanisms. By producing a sharply delineated region within which the reorganization takes place, we can topographically distinguish this area from the source of visual input to the region undergoing recovery, and characterize the changes in axonal arbors of neurons within and outside the LPZ. Previously, we have demonstrated that excitatory horizontal connections undergo substantial sprouting over the course of reorganization (Darian-Smith and Gilbert, 1994; Yamahachi et al., 2009; Marik et al., 2010). In the current study, we explore the involvement of inhibitory connections in the remapping and their relationship to the excitatory neurons sprouting into the LPZ.

While excitatory neurons have been the main focus of adult experience-dependent plasticity, there is growing evidence that inhibitory neurons also play a role. Sensory stimulation and learning lead to an increase of inhibitory neuron synapses on excitatory neuron spines (Knott et al., 2002; Jasinska et al., 2010). Retinal lesions and ocular dominance plasticity in the adult are associated with a loss of inhibitory synapses (Keck et al., 2011; van Versendaal et al., 2012). Furthermore, there is evidence that the dendrites of inhibitory neurons are structurally and functionally modifiable (Lee et al., 2006; Kameyama et al., 2010; Chen et al., 2011). In the current study, we sought to determine the extent of inhibitory axonal remodeling within and around the LPZ. To track the changes, we have used genetically engineered recombinant adeno-associated virus (AAV) to provide cell type-specific labeling. Our studies show extensive outgrowth of inhibitory axons along with pruning following the placement of retinal lesions.

Materials and Methods

Viral injections. All AAV injections and two-photon imaging sessions were performed as previously described (Stettler et al., 2006; Yamahachi et al., 2009). Two anesthetized adult male primates were used for the experiments (Macaca fascicularis). All procedures were performed according to institutional and federal guidelines.

We genetically engineered a recombinant AAV construct to label inhibitory neurons by using a 2.7 bp DNA fragment directly upstream from

Received Oct. 10, 2013; revised Nov. 27, 2013; accepted Dec. 15, 2013.

Author contributions: S.A.M., H.Y., and C.D.G. designed research; S.A.M., H.Y., S.M.Z.A.B., and C.D.G. performed research; S.A.M., H.Y., and C.D.G. analyzed data; S.A.M., H.Y., S.M.Z.A.B., and C.D.G. wrote the paper.

This work was supported by National Institutes of Health Grant EY018119.

The authors declare no competing financial interests.

Correspondence should be addressed to Charles D. Gilbert, Laboratory of Neurobiology, The Rockefeller University, 1230 York Avenue, New York, NY 10065. E-mail: gilbert@rockefeller.edu.

H. Yamahachi's present address: Kavli Institute for Systems Neuroscience/Centre for Neural Computation, Norwegian University of Science and Technology, NO-7491 Trondheim, Norway.

DOI:10.1523/JNEUROSCI.4345-13.2014

 0270-6474/14/341625-08$15.00/0

the *GAD65* gene, as previously described (Marik et al., 2010). The titer was determined to be 2×10^{13} particles/ml by quantitative PCR using GFP-specific primers. We confirmed the specificity of labeling for inhibitory neurons by immunohistochemistry, using a cocktail of antibodies against calbindin (1:5000), calretinin (1:2000), and parvalbumin (1:5000; Swant) that collectively label 90% of all inhibitory neurons (Seress et al., 1993; Heizmann and Braun, 1995; del Río and DeFelipe, 1996). Sections were incubated for 1 h in 10% normal goat serum and 0.2% Triton X-100 in Tris-buffered saline (TBS) solution, followed by 48 h of incubation of primary antibodies; rinsed three times in TBS; and then incubated with a secondary antibody TRITC goat anti-rabbit (1:500; Jackson ImmunoResearch Laboratories) at room temperature for 2 h. After the rinsing, the sections were mounted and coverslipped with Vectashield with DAPI (Vector Laboratories).

Dexamethasone (0.25 mg/kg) was administered the night before making injections of virus. The initial induction of anesthesia was done using ketamine (10 mg/kg body weight). A venous cannula was inserted, and the animal was intubated with an endotracheal tube. Anesthesia was maintained with isoflurane (3% induction, 1–1.5% maintenance) throughout surgery. All vital signs were monitored and recorded throughout the experiment. For the viral injection surgery, animals were placed in a stereotactic frame. Under sterile surgical conditions an incision was made, the scalp retracted, and a craniotomy measuring 6×14 mm was made directly over the V1/V2 border. An H-cut was made in the dura, and the dura was held back for viral injections. Electrodes made from borosilicate glass (World Precision Instruments) were pulled, and the tip was beveled before gas sterilization and surgery. We pressure injected 200 nl of AAV-GAD65.EGFP per injection site over several minutes using a Picospritzer III (Parker Hannifin). Two medial-lateral rows of three to four injections were made parallel to the V1/V2 border. There was more space between injections in the middle of the craniotomy to allow for the later placement of the LPZ boundary during the retinal lesions. A piece of artificial dura (Kwik Sil, World Precision Instruments) was slipped under the dura, and the dura was sutured. The bone was replaced and secured with a metal mesh and three screws. Bone wax was applied to the four sides. The scalp was closed and sutured back into place. After the surgery, the animal returned to its cage where it remained for at least three months before the onset of imaging.

In vivo *imaging.* The week before the onset of imaging sessions a head post and chamber were implanted as in Yamahachi et al. (2009). Anesthesia and surgery were performed in a similar manner to the injection surgery. Additionally, a craniotomy (16 mm in diameter) was made over the area of cortex in which the viral injections had been made. A quartz coverslip embedded in Kwik Sil, mounted in place by titanium rings, was used to reduce motion artifacts, protect the cortex, and reduce dural regrowth. The chamber was closed and sealed between imaging sessions, allowing us to conduct multiple imaging sessions extending over several weeks before and after making the lesions. Imaging sessions were conducted under anesthesia.

Images were collected as described in the studies by Stettler et al. (2006) and Yamahachi et al. (2009) on a custom-built two-photon microscope that was modified from a Leica TCS Sp2 confocal microscope with a custom moveable scanning head, which can be moved in three dimensions using a Sutter MP-285–3Z micromanipulator. The laser source was provided by a Ti-sapphire laser (Tsunami/Millenia System, Spectra-Physics). Images were acquired with Leica Confocal software. Images were taken with a 40× water-immersion objective (FLUOR 40×/0.8 W DIC M, Nikon).

z-stacks were collected from superficial cortical layers before and for 3 weeks after the retinal lesion was made. Each stack measured 250×250 μm in *x* and *y*, and 300 μm in *z*. As many injection sites were imaged as the maximum length of anesthesia of the animal allowed. Since a large area needed to be covered for these imaging sessions, we were not able to return to every injection site at every imaging session. We reconstructed and analyzed a total axon length of 230.5 mm for these experiments.

Mapping RF and retinal lesions. Receptive field mapping and retinal lesion methods have been described previously (Darian-Smith and Gilbert, 1995; Yamahachi et al., 2009). After 2 weeks of baseline imaging, we mapped the RFs of the cortical area of interest using an insulated tungsten microelectrode (impedance 1–2 MΩ; Alpha Omega). Superficial electrode penetrations were evenly spaced, avoiding areas to be imaged to prevent damage. A hand-held light stimulator was used to map minimum response fields, orientation preference, and ocular dominance.

Retinal lesions were made as described previously (Gilbert and Wiesel, 1990, 1992; Yamahachi et al., 2009). After RF mapping was completed, the microelectrode was placed at the desired LPZ border location within the chamber. The lesion was placed so that the LPZ boundary was located at the center of the chamber and between injection sites, with the nearest injection sites located 1 mm from the boundary. The area of the retina that corresponded to the location of the microelectrode was determined by using the guide light from an ophthalmic laser (IRIDEX) as a visual stimulus. Binocular retinal lesions were made by diode laser delivering 300 mW for 800–1000 ms. The position of the LPZ was confirmed by subsequent electrophysiological mapping.

Image analysis. Off-line images were viewed with ImageJ (http://rsbweb.nih.gov/ij/). Images were deconvolved using Huygens deconvolution software (Scientific Volume Imaging). Finally, axons were traced via the semiautomatic mode in Neuromantic (version 1.6.3; http://www.rdg.ac.uk/neuromantic) using image stacks. Tracings were manually confirmed, and reconstructions for different time points were performed in parallel at the same cortical location for consecutive time points. Axonal tracing was quantified using Neuromantic and Matlab software. The area was determined by tracing the outer edge of the axons reconstructed in manual mode of Neuromantic, which produces an swc file. The area was calculated by a Matlab program that measures the area circumscribed by the points in the swc file.

Results

Our study of the structural plasticity of inhibitory neurons following retinal lesions involved a combination of cell type-specific fluorescent labeling of inhibitory neurons and *in vivo* two-photon imaging. We genetically engineered an AAV to label inhibitory neurons within primary visual cortex by placing EGFP expression under the control of a portion of the GAD65 promoter (AAV-GAD65.EGFP). The specificity of GFP expression for inhibitory neurons was confirmed using a cocktail of antibodies against calbindin, calretinin, and parvalbumin, which labels 90% of all inhibitory neurons (Fig. 1*C*). Of the neurons expressing GFP, 88% also expressed one of the three calcium-binding proteins ($N = 365$). The soma size of the 12% of non-colocalized neurons ranged from 9 to 15 μm in diameter, suggesting that they were also inhibitory neurons (Kawaguchi, 1995; Lübke et al., 1996). Since the GAD65 virus labels nearly all inhibitory neurons, it does not permit one to differentiate the projections of different subtypes of inhibitory neurons, and the density of labeling at the injection site does not allow one to classify the labeled cells on morphological grounds. However, the longest range axons, which constitute the majority of the collaterals in the reconstruction, are likely to originate from basket cells, which form the longest range axonal arbors among inhibitory neurons (Buzás et al., 2001). The GAD65 virus was pressure injected in two rows of three to four injections that were distributed along the medial–lateral axis, parallel to the V1/V2 border (Fig. 1*B*). The first imaging session was performed at least 3 months after the injections to ensure that all virally infected neurons were fully labeled. We used two-photon microscopy to image labeled inhibitory neurons before and after making focal binocular retinal lesions. We mapped the RFs of neurons at multiple locations on the opercular surface of Macaque V1 to guide the placement of lesions and imaged regions. The same procedures were performed on two different monkeys with similar results. To assess the stability of axonal arbors under normal conditions, we imaged the same region of cortex over multiple time points before making the lesion. The retinal lesion was then placed such that half of the

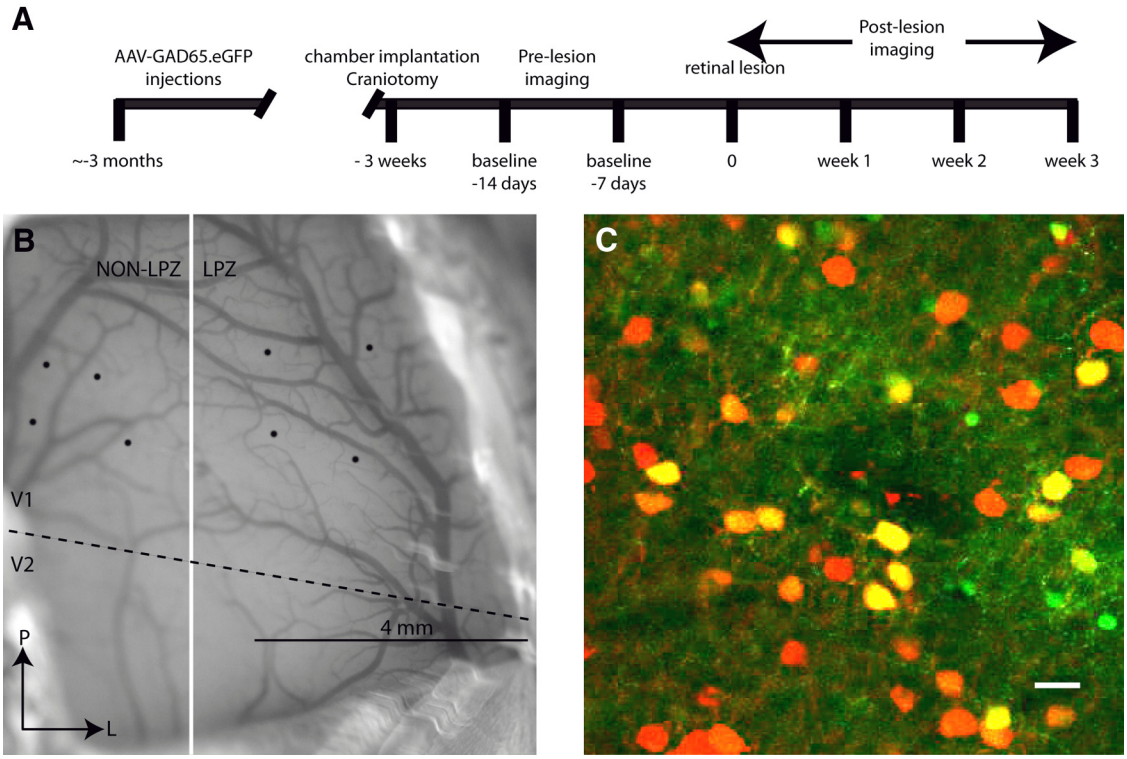

Figure 1. Experimental design. ***A***, Time line showing the experimental protocol. ***B***, Diagram showing the location of injections for one representative monkey. V1/V2 border is depicted by a dashed black line, and the future location of the lesion projection border is depicted by a white line. Scale bar, 4 mm. ***C***, Representative injection site from a transverse section of macaque V1 with neurons labeled with AAV-GAD65.EGFP (green) and immunostained with antibodies against calbindin, calretinin, and parvalbumin (red). Neurons with both GFP expression and immunostaining are yellow. Scale bar, 15 μm.

injections were in the LPZ and half in the peri-LPZ (the cortical region surrounding the LPZ), which allowed us to directly compare structural changes of inhibitory neurons lying in cortical areas undergoing reorganization of retinotopic maps with those that had retained visual input throughout the postlesion period (Fig. 1).

Axonal dynamics during normal experience

Axonal arbors of inhibitory neurons were imaged repeatedly to determine the basal level of axonal dynamics during normal visual experience. Selected cortical areas containing labeled inhibitory axons were imaged in two sessions separated by 1 week. A total axon length of 8 mm was reconstructed in this region (Fig. 2). Over this period, axonal arbors of inhibitory neurons were stable, showing no significant change in total length ($p = 0.57$, paired t test; 3% change between the two baseline sessions). The total axonal length reconstructed for control injection sites at baseline − 14 d was 4010 μm, and at baseline − 7 d was 3960 μm. While the axonal arbors were stable under these conditions, there was bouton turnover at a rate of 10% per week.

Axonal dynamics within the LPZ following retinal lesions

In contrast to their stability under normal conditions, inhibitory axons underwent significant growth and pruning within the LPZ following the making of retinal lesions (ANOVA, $p = 0.03$). Inhibitory neurons located within the LPZ were imaged on the day of and at 3 weeks following the making of the retinal lesion. We reconstructed a total length of 160 mm of axonal arbors within the LPZ of two monkeys. In monkey A, there was rapid axonal growth and pruning of neurons located in the LPZ within hours of making the lesion (Fig. 3*B*). Following the making of the lesion, 49% of the axonal arbor was pruned back. Considerable axonal sprouting occurred even on the day on which the retinal lesion was made (65% increase in length compared with baseline). Axonal sprouting continued to occur for the duration of our imaging sessions, which extended over 3 weeks (387% increase in axon length at 3 weeks postlesion; Fig. 3*A*,*B*). At 3 weeks after the lesion was made, monkey A had 57% of its original axons pruned back while adding over twice the axonal length present at baseline (223%). In monkey B at 3 weeks, 42% of the original axonal arbor was pruned back, and there was considerable axonal growth (550% increase in length compared with baseline). The axons after the lesion was made induced changes that were longer than those present at baseline and significantly increased the territory that they occupied within the LPZ (baseline, 0.09 mm^2; postlesion, 0.77 mm^2; $p < 0.001$; Fig. 4*A*). The lateral extent was measured by measuring the axon arbors from tip to tip in the widest dimension, though these arbors did not uniformly increase in all directions. Instead, their greatest increase was directed toward the LPZ border. The lateral extent of axonal arbors that we imaged went from 425 to 4490 μm. For the injection sites that were the closest to the LPZ border, 10% of the newly sprouted axons extended on average 563 ± 110 μm over the LPZ border into the peri-LPZ. While axonal growth expanded the cortical territory that these inhibitory neurons occupied, the overall axonal density decreased to 43% of original baseline density at 3 weeks after the lesion was made (Fig. 4*B*).

Axonal dynamics within the peri-LPZ following retinal lesions

Axons of neurons located in the peri-LPZ were imaged at 2 and 3 weeks after making the retinal lesion. Sixty-five millimeters of

axonal arbors were reconstructed from four injection sites for the peri-LPZ experiments. Axons imaged at different time points were compared against baseline imaging sessions. Axons within the peri-LPZ underwent axonal growth and axonal pruning (Fig. 3). Axonal growth increased substantially between week 2 (14% from baseline) and week 3 (137% from baseline; Fig. 3*C*). While there was axonal growth within the peri-LPZ, it progressed more slowly than in the LPZ, and none of the new growth within the peri-LPZ extended over the LPZ border into the LPZ. Thirty-seven percent of the original axons imaged during baseline were pruned by 2 weeks after the retinal lesion was made. Compared with controls, axonal growth and pruning were elevated within the peri-LPZ (t test: retracted, $p < 0.01$; added, $p = 0.05$). Axonal sprouting was already evident at the earliest time that we examined (2 weeks, 14%). Although there was a significant amount of new axonal growth within the peri-LPZ, the area that the axons occupied did not significantly increase (baseline, 0.2 mm^2; postlesion, 0.4 mm^2; t test, $p = 0.69$; Fig. 4*A*). The new growth was counterbalanced with axonal pruning since the axonal density of imaged axons did not significantly increase within the peri-LPZ (t test, $p = 0.64$).

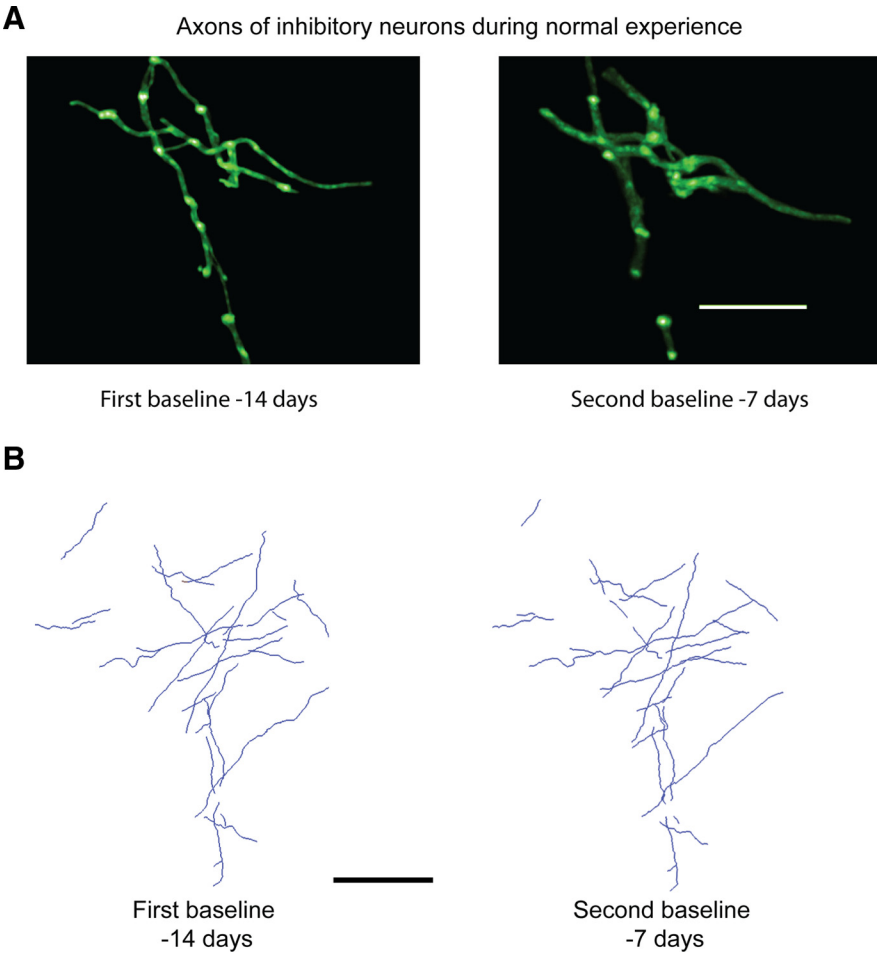

Figure 2. Axons of inhibitory neurons during normal visual experience. ***A***, *z*-projection of inhibitory neurons labeled with AAV-GAD65.EGFP in monkey V1 during two control imaging sessions. Note that the bright spots are boutons, a small percentage of which are recycled over the course of a week. Scale bar, 25 μm. ***B***, Reconstruction of one injection site on two different baseline imaging sessions. Scale bar, 100 μm.

Location in relationship to LPZ border

To determine the influence of the position of the labeled peri-LPZ inhibitory neurons with respect to the LPZ border on the amount of axonal restructuring, the sites of LPZ injections were grouped into one of two groups: those located <1 mm from LPZ border and those located >1 mm from LPZ border. For each group, we calculated the percentage change in axonal length. Similar levels of pruning were seen for injection sites within 1 mm of the LPZ border (mean distance, 0.8 mm) as for those >1 mm from the LPZ border (mean distance, 1.7 mm). The amount of axonal growth, however, depended on the distance of the projecting neurons from the LPZ border. Injections that were farther from the LPZ border underwent more axonal growth (231% increase in axonal length) than the injections that were closer (146% increase in axonal length). The axons of neurons located within 1 mm of the LPZ border sprouted over the border, extending several hundred micrometers into the peri-LPZ. The axons that expanded into the peri-LPZ made up 10% of the newly sprouted axons. Notably, inhibitory neuron axons within the peri-LPZ, at an equivalent distance from the LPZ border, did not extend beyond the LPZ border.

Discussion

The changes in the arbors of inhibitory neurons in the LPZ following the making of retinal lesions were rapid and extensive. Previous work on excitatory axons showed similar effects, with exuberant outgrowth and a parallel process of pruning (Yamahachi et al., 2009; Marik et al., 2010). Dendritic arbors also undergo anatomical changes in response to experience-dependent plasticity (Hickmott and Steen, 2005; Cheetham et al., 2008). Numerous *in vivo* studies have demonstrated changes at the synaptic level. Experience-dependent plasticity is associated with an increase in both dendritic spines and axonal boutons (Trachtenberg et al., 2002; Holtmaat et al., 2006; Keck et al., 2008; Hofer et al., 2009; Xu et al., 2009; Yang et al., 2009; Marik et al., 2010; Wilbrecht et al., 2010; Fu et al., 2012). Together, these data suggest that experience-dependent plasticity, especially that associated with remapping of cortical topography, is associated with changes in both inhibitory and excitatory connections. We report here at baseline, in the absence of modifications of sensory experience, both excitatory and inhibitory axonal arbors are relatively quiescent, but show ongoing activity of synaptic turnover, as reflected by the formation and retraction of axonal boutons, turning over at a rate of 10% per week, without major changes in axon collaterals. After placement of retinal lesions, axonal remodeling becomes sharply and dramatically upregulated. Over time, the density of excitatory axonal projections from the peri-LPZ to the LPZ increases, which may account for the reorganization of the retinotopic map and the shift in RFs among LPZ neurons. Similarly, for inhibitory neurons, the most pronounced axonal changes were seen within the LPZ, mirroring the effects observed for peri-LPZ excitatory neurons. One difference, however, was the increase in cortical area occupied by the inhibitory axons,

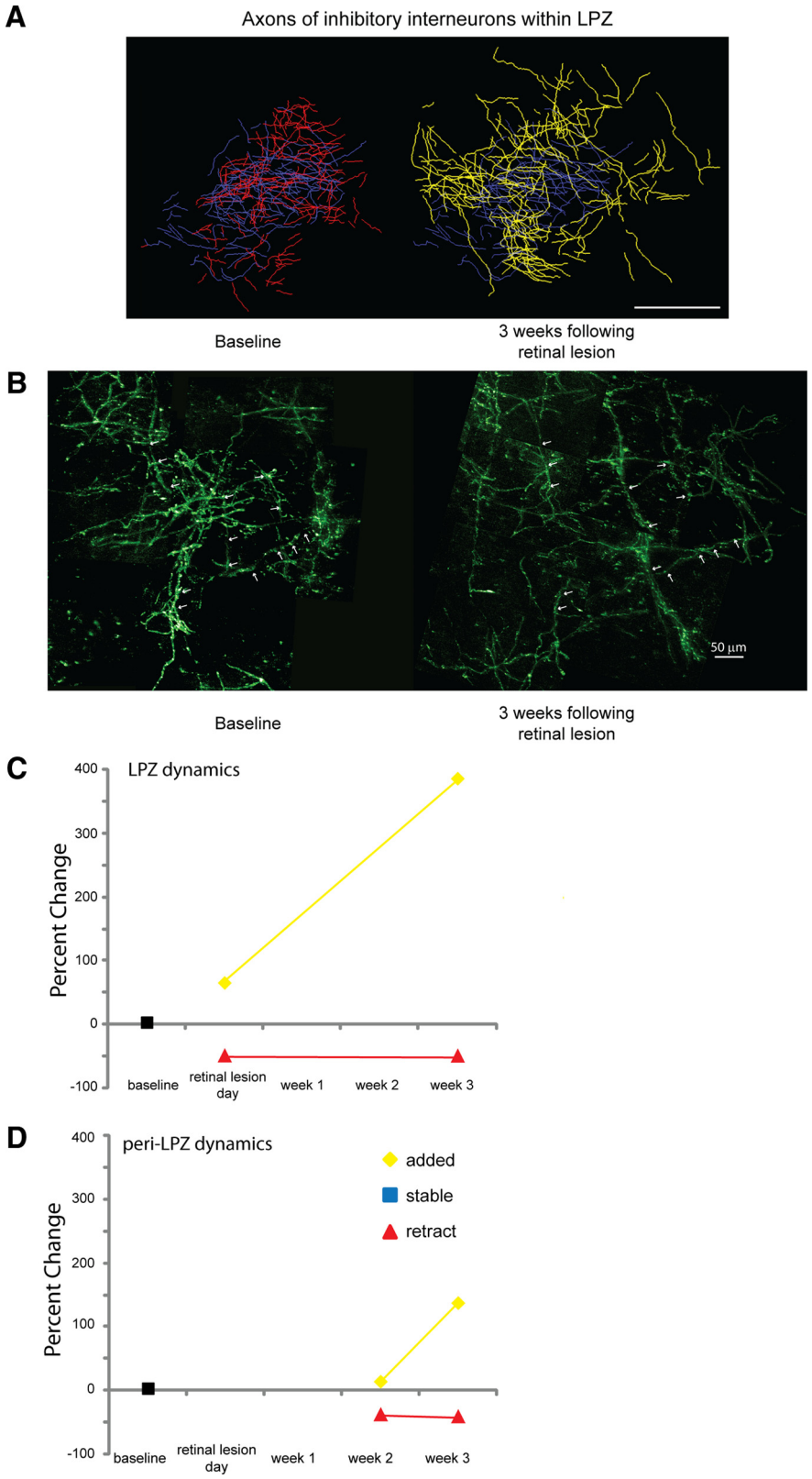

Figure 3. Inhibitory neurons axonal dynamics. ***A***, Color-coded reconstructed axonal arbors located within the LPZ. Blue, Stable; yellow, added; red, retracted. Scale bar, 100 μm. ***B***, Axons of inhibitory neurons within the LPZ. *z*-projections of labeled imaged axons at baseline imaging sessions and 3 weeks following the retinal lesion. Arrows depict a couple of example axons that were present at both time points. Note the decrease in the axonal density and the expansion of the area the axons occupy following axonal sprouting. Scale bar, 50 μm. ***C***, Quantification of LPZ dynamics; the percentage of axons that were added, retracted, or remained stable compared with baseline imaging sessions for axons of inhibitory neurons located within the LPZ. ***D***, Quantification of peri-LPZ dynamics. Percentage of axons that were added, retracted, or remained stable compared with baseline imaging sessions for axons of inhibitory neurons located within the peri-LPZ.

which extended far beyond their normal territory, with many crossing the LPZ boundary into the peri-LPZ. Our findings complement earlier studies showing remodeling of inhibitory dendrites (changing 5–8% in length under conditions of normal experience; Lee et al., 2006), though here we showed that the axons could change on the order of several hundred percent. There is also precedent for inhibitory neurons to undergo robust structural changes following alteration in experience. The whisker map of mouse somatosensory cortex is remapped following whisker plucking, with the cortical area originally responding to the plucked whiskers becoming activated instead by the adjacent row of whiskers. Under these conditions, the axons of inhibitory neurons located in the cortical area originally representing the plucked whiskers (the somatosensory LPZ) undergo similar massive axonal reorganization (Marik et al., 2010). This study demonstrates that the axonal plasticity is conserved through evolution and across sensory areas.

Several characteristics of the axonal changes are reminiscent of the physiology of the remapping of topography following the making of lesions of the sensory periphery. On the same day that retinal lesions are made, RFs of neurons located just within the LPZ boundary shift to positions outside the retinal scotoma (Gilbert and Wiesel, 1992). This is reflected in the rapid initial changes in axonal arbors. The map reorganization can extend for ~8 mm across the LPZ, approximating the extent of long-range horizontal connections (Gilbert, 1992). Over a period of months, the recovery of visual responses propagates toward the center of the LPZ, which may reflect an enrichment of the clusters of axon collaterals within the preexisting network of long-range horizontal connections, which extend for many millimeters from the cell bodies giving rise to these connections. Some studies indicate fill-in of LPZ activity over larger distances, which is indicative of the sprouting of excitatory horizontal connections that extend beyond the normal envelope of the territory they cover (Florence et al., 1998). Putting aside the capacity for excitatory axons to change their range, in the current study we saw a substantial increase in the envelope of coverage by inhibitory axons. Though there has been some question as to the nature of the reorganization of functional maps (Smirnakis et al., 2005), the many physiological and anatomical studies demonstrating the phenomenon (Gilbert et al., 1990; Kaas et al., 1990; Hei-

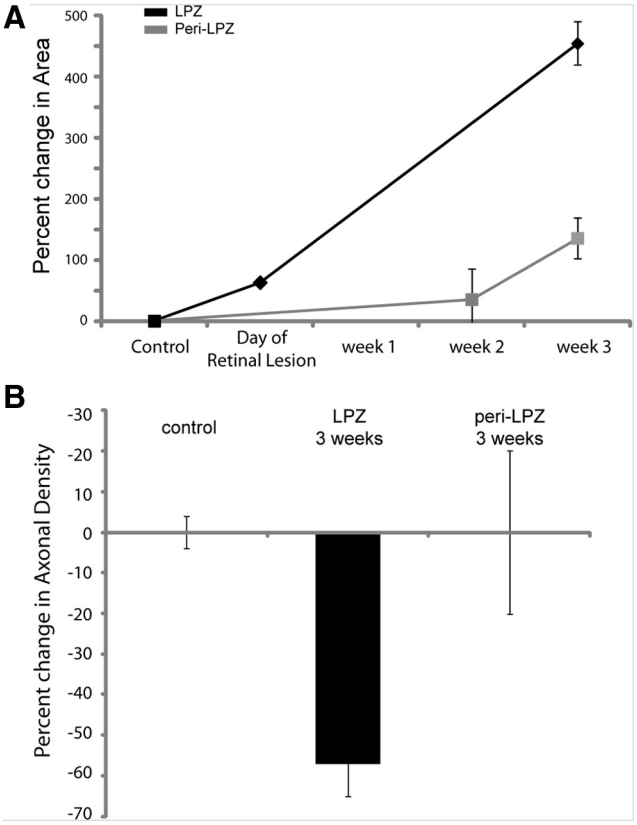

Figure 4. Area occupied by inhibitory neurons. ***A***, Graph depicting the percentage change in the area occupied by axons of inhibitory neurons. LPZ, Black; peri-LPZ, gray. ***B***, Bar graph depicting the change in axonal density from baseline for control (both baseline sessions), as well as, LPZ and peri-LPZ at 3 weeks after the making of the lesion.

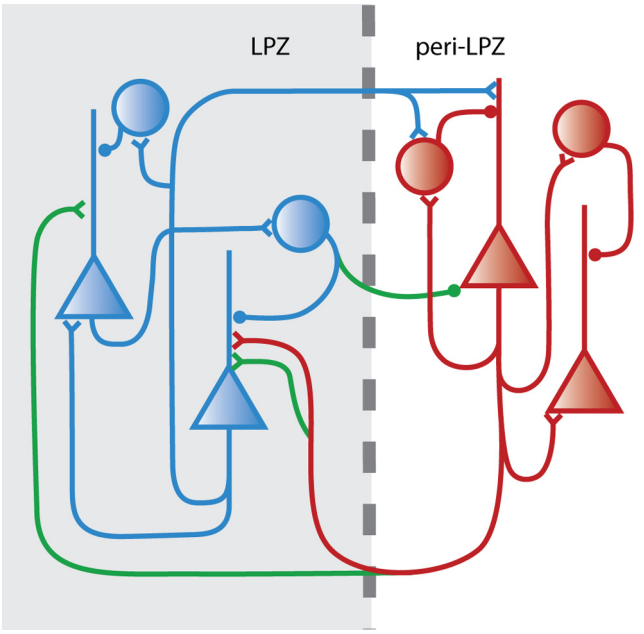

Figure 5. The reciprocal changes in inhibitory and excitatory arbors during experience-dependent cortical plasticity maintains the E–I balance in cortical circuits. This schematic representation of the current findings and those of our previous study on excitatory axons (Yamahachi et al., 2009) shows excitatory neurons (triangles) within the peri-LPZ that extend new axons (green) into the LPZ (shaded area) and inhibitory neurons (circles) within the LPZ, extending axons in the reverse direction, toward the peri-LPZ.

nen and Skavenski, 1991; Chino et al., 1995; Calford et al., 2000, 2005; Baker et al., 2005, 2008; Giannikopoulos and Eysel, 2006; Yamahachi et al., 2009; Marik et al., 2010), including the current study, support the idea that the adult sensory cortex is capable of undergoing substantial experience-dependent change, with LPZ fill-in extending up to a maximum of 8–10 mm.

The changes in inhibitory connections are important for understanding the link between alterations of cortical activity and changes in different elements of cortical circuits. In addition, the changes may reflect the requirement for cortical circuits to maintain excitatory–inhibitory (E–I) balance (Giannikopoulos and Eysel, 2006). During development, the maturation of inhibition is associated with the duration and cessation of critical period plasticity (Hensch and Fagiolini, 2005; Di Cristo et al., 2007; Sugiyama et al., 2008). In early postnatal development, excitation and inhibition become balanced as the cortex matures (Dorrn et al., 2010). The balance between inhibition and excitation maintains network stability, with excitatory and inhibitory synaptic inputs showing similar tuning (Ferster, 1986; Troyer et al., 1998; van Vreeswijk and Sompolinsky, 1998; Anderson et al., 2000; Wehr and Zador, 2003; Tan et al., 2004; Priebe and Ferster, 2005, 2006; Ozeki et al., 2009). In the auditory system, retuning of RFs increases excitation to the paired stimulus and is followed over time by an increase in inhibition that balances the excitation, ultimately contributing to the changed preferred frequency (Froemke et al., 2007). Previous retinal lesion studies have demonstrated that there is a decrease in immunoreactivity to GAD within the LPZ, while there is an increase in GAD and GABA in the peri-LPZ (Rosier et al., 1995; Massie et al., 2003). Our study corroborates these findings with the observation of extensive axonal pruning at early time points within the LPZ along with axonal growth that extends over the LPZ border. Axonal growth increases the territory that the axons of inhibitory neurons occupy, but there is a decrease in density of their arbors. We hypothesize that axons of inhibitory neurons that extend over the LPZ/peri-LPZ border may target the peri-LPZ excitatory neurons that send new axonal projections into the LPZ (Fig. 5). This requires verification at the ultrastructural level. The change in inhibitory circuits seen in the current study may reflect the requirement for maintaining E–I balance, whereby inhibitory neurons project out of the LPZ to contact the peri-LPZ neurons that provide the increased excitatory drive to the LPZ.

The functional remapping of cortical topography in response to changes in experience is a ubiquitous phenomenon that is observed across many different species, including humans (Rose et al., 1960; Merzenich et al., 1983a,b, 1984; Simons and Land, 1987; Clark et al., 1988; Sanes et al., 1988, 1990; Robertson and Irvine, 1989; Cusick et al., 1990; Gilbert et al., 1990; Kaas et al., 1990; Heinen and Skavenski, 1991; Ramachandran and Gregory, 1991; Fox, 1992; Gilbert and Wiesel, 1992; Diamond et al., 1993; Recanzone et al., 1993; Weinberger et al., 1993; Darian-Smith and Gilbert, 1994, 1995; Chino et al., 1995; Das and Gilbert, 1995a; Elbert et al., 1995; Flor et al., 1995; Schmid et al., 1996; Wallace and Fox, 1999; Calford et al., 2000, 2003; Mataga et al., 2004; Baker et al., 2005, 2008; Giannikopoulos and Eysel, 2006; Keck et al., 2008; Dilks et al., 2009; Makin et al., 2013). The remapping seen following peripheral lesions may recruit processes that operate under normal experience, such as that observed during perceptual learning

References

Anderson JS, Carandini M, Ferster D (2000) Orientation tuning of input conductance, excitation, and inhibition in cat primary visual cortex. J Neurophysiol 84:909–926. Medline

Baker CI, Peli E, Knouf N, Kanwisher NG (2005) Reorganization of visual processing in macular degeneration. J Neurosci 25:614–618. CrossRef Medline

Baker CI, Dilks DD, Peli E, Kanwisher N (2008) Reorganization of visual processing in macular degeneration: replication and clues about the role of foveal loss. Vision Res 48:1910–1919. CrossRef Medline

Buzás P, Eysel UT, Adorján P, Kisvárday ZF (2001) Axonal topography of cortical basket cells in relation to orientation, direction, and ocular dominance maps. J Comp Neurol 437:259–285. CrossRef Medline

Calford MB, Wang C, Taglianetti V, Waleszczyk WJ, Burke W, Dreher B (2000) Plasticity in adult cat visual cortex (area 17) following circumscribed monocular lesions of all retinal layers. J Physiol 524:587–602. CrossRef Medline

Calford MB, Wright LL, Metha AB, Taglianetti V (2003) Topographic plasticity in primary visual cortex is mediated by local corticocortical connections. J Neurosci 23:6434–6442. Medline

Calford MB, Chino YM, Das A, Eysel UT, Gilbert CD, Heinen SJ, Kaas JH, Ullman S (2005) Neuroscience: rewiring the adult brain. Nature 438:E3. CrossRef Medline

Cheetham CE, Hammond MS, McFarlane R, Finnerty GT (2008) Altered sensory experience induces targeted rewiring of local excitatory connections in mature neocortex. J Neurosci 28:9249–9260. CrossRef Medline

Chen JL, Flanders GH, Lee WC, Lin WC, Nedivi E (2011) Inhibitory dendrite dynamics as a general feature of the adult cortical microcircuit. J Neurosci 31:12437–12443. CrossRef Medline

Chino YM, Smith EL 3rd, Kaas JH, Sasaki Y, Cheng H (1995) Receptive-field properties of deafferentated visual cortical neurons after topographic map reorganization in adult cats. J Neurosci 15:2417–2433. Medline

Clark SA, Allard T, Jenkins WM, Merzenich MM (1988) Receptive fields in the body-surface map in adult cortex defined by temporally correlated inputs. Nature 332:444–445. CrossRef Medline

Cusick CG, Wall JT, Whiting JH Jr, Wiley RG (1990) Temporal progression of cortical reorganization following nerve injury. Brain Res 537:355–358. CrossRef Medline

Darian-Smith C, Gilbert CD (1994) Axonal sprouting accompanies functional reorganization in adult cat striate cortex. Nature 368:737–740. CrossRef Medline

Darian-Smith C, Gilbert CD (1995) Topographic reorganization in the striate cortex of the adult cat and monkey is cortically mediated. J Neurosci 15:1631–1647. Medline

Das A, Gilbert CD (1995a) Long-range horizontal connections and their role in cortical reorganization revealed by optical recording of cat primary visual cortex. Nature 375:780–784. CrossRef Medline

Das A, Gilbert CD (1995b) Receptive field expansion in adult visual cortex is linked to dynamic changes in strength of cortical connections. J Neurophysiol 74:779–792. Medline

del Río MR, DeFelipe J (1996) Colocalization of calbindin D-28k, calretinin, and GABA immunoreactivities in neurons of the human temporal cortex. J Comp Neurol 369:472–482. CrossRef Medline

Diamond ME, Armstrong-James M, Ebner FF (1993) Experience-dependent plasticity in adult rat barrel cortex. Proc Natl Acad Sci U S A 90:2082–2086. CrossRef Medline

Di Cristo G, Chattopadhyaya B, Kuhlman SJ, Fu Y, Bélanger MC, Wu CZ, Rutishauser U, Maffei L, Huang ZJ (2007) Activity-dependent PSA expression regulates inhibitory maturation and onset of critical period plasticity. Nat Neurosci 10:1569–1577. CrossRef Medline

Dilks DD, Baker CI, Liu Y, Kanwisher N (2009) "Referred visual sensations": rapid perceptual elongation after visual cortical deprivation. J Neurosci 29:8960–8964. CrossRef Medline

Dorrn AL, Yuan K, Barker AJ, Schreiner CE, Froemke RC (2010) Developmental sensory experience balances cortical excitation and inhibition. Nature 465:932–936. CrossRef Medline

Elbert T, Pantev C, Wienbruch C, Rockstroh B, Taub E (1995) Increased cortical representation of the fingers of the left hand in string players. Science 270:305–307. CrossRef Medline

Ferster D (1986) Orientation selectivity of synaptic potentials in neurons of cat primary visual cortex. J Neurosci 6:1284–1301. Medline

Flor H, Elbert T, Knecht S, Wienbruch C, Pantev C, Birbaumer N, Larbig W, Taub E (1995) Phantom-limb pain as a perceptual correlate of cortical reorganization following arm amputation. Nature 375:482–484. CrossRef Medline

Florence SL, Taub HB, Kaas JH (1998) Large-scale sprouting of cortical connections after peripheral injury in adult macaque monkeys. Science 282:1117–1121. CrossRef Medline

Fox K (1992) A critical period for experience-dependent synaptic plasticity in rat barrel cortex. J Neurosci 12:1826–1838. Medline

Froemke RC, Merzenich MM, Schreiner CE (2007) A synaptic memory trace for cortical receptive field plasticity. Nature 450:425–429. CrossRef Medline

Fu M, Yu X, Lu J, Zuo Y (2012) Repetitive motor learning induces coordinated formation of clustered dendritic spines in vivo. Nature 483:92–95. CrossRef Medline

Giannikopoulos DV, Eysel UT (2006) Dynamics and specificity of cortical map reorganization after retinal lesions. Proc Natl Acad Sci U S A 103:10805–10810. CrossRef Medline

Gilbert CD (1992) Horizontal integration and cortical dynamics. Neuron 9:1–13. CrossRef Medline

Gilbert CD, Wiesel TN (1990) The influence of contextual stimuli on the orientation selectivity of cells in primary visual cortex of the cat. Vision Res 30:1689–1701. CrossRef Medline

Gilbert CD, Wiesel TN (1992) Receptive field dynamics in adult primary visual cortex. Nature 356:150–152. CrossRef Medline

Gilbert CD, Hirsch JA, Wiesel TN (1990) Lateral interactions in visual cortex. Cold Spring Harb Symp Quant Biol 55:663–677. CrossRef Medline

Heinen SJ, Skavenski AA (1991) Recovery of visual responses in foveal V1 neurons following bilateral foveal lesions in adult monkey. Exp Brain Res 83:670–674. Medline

Heizmann CW, Braun K (1995) Localization of EF-hand Ca2+-binding proteins in the CNS. In: Calcium regulation by calcium-binding proteins in neurodegenerative disorders. Austin, TX: Springer.

Hensch TK, Fagiolini M (2005) Excitatory-inhibitory balance and critical period plasticity in developing visual cortex. Prog Brain Res 147:115–124. CrossRef Medline

Hickmott PW, Steen PA (2005) Large-scale changes in dendritic structure during reorganization of adult somatosensory cortex. Nat Neurosci 8:140–142. CrossRef Medline

Hofer SB, Mrsic-Flogel TD, Bonhoeffer T, Hübener M (2009) Experience leaves a lasting structural trace in cortical circuits. Nature 457:313–317. CrossRef Medline

Holtmaat A, Wilbrecht L, Knott GW, Welker E, Svoboda K (2006) Experience-dependent and cell-type-specific spine growth in the neocortex. Nature 441:979–983. CrossRef Medline

Jasinska M, Siucinska E, Cybulska-Klosowicz A, Pyza E, Furness DN, Kossut M, Glazewski S (2010) Rapid, learning-induced inhibitory synaptogenesis in murine barrel field. J Neurosci 30:1176–1184. CrossRef Medline

Kaas JH, Krubitzer LA, Chino YM, Langston AL, Polley EH, Blair N (1990) Reorganization of retinotopic cortical maps in adult mammals after lesions of the retina. Science 248:229–231. CrossRef Medline

Kameyama K, Sohya K, Ebina T, Fukuda A, Yanagawa Y, Tsumoto T (2010) Difference in binocularity and ocular dominance plasticity between GABAergic and excitatory cortical neurons. J Neurosci 30:1551–1559. CrossRef Medline

Kawaguchi Y (1995) Physiological subgroups of nonpyramidal cells with specific morphological characteristics in layer II/III of rat frontal cortex. J Neurosci 15:2638–2655. Medline

Keck T, Mrsic-Flogel TD, Vaz Afonso M, Eysel UT, Bonhoeffer T, Hübener M (2008) Massive restructuring of neuronal circuits during functional reorganization of adult visual cortex. Nat Neurosci 11:1162–1167. CrossRef Medline

Keck T, Scheuss V, Jacobsen RI, Wierenga CJ, Eysel UT, Bonhoeffer T, Hübener M (2011) Loss of sensory input causes rapid structural changes of inhibitory neurons in adult mouse visual cortex. Neuron 71:869–882. CrossRef Medline

Knott GW, Quairiaux C, Genoud C, Welker E (2002) Formation of dendritic spines with GABAergic synapses induced by whisker stimulation in adult mice. Neuron 34:265–273. CrossRef Medline

Lee WC, Huang H, Feng G, Sanes JR, Brown EN, So PT, Nedivi E (2006) Dynamic remodeling of dendritic arbors in GABAergic interneurons of adult visual cortex. PLoS Biol 4:e29. CrossRef Medline

Lübke J, Markram H, Frotscher M, Sakmann B (1996) Frequency and dendritic distribution of autapses established by layer 5 pyramidal neurons in the developing rat neocortex: comparison with synaptic innervation of adjacent neurons of the same class. J Neurosci 16:3209–3218. Medline

Makin TR, Scholz J, Filippini N, Henderson Slater D, Tracey I, Johansen-Berg

H (2013) Phantom pain is associated with preserved structure and function in the former hand area. Nat Commun 4:1570. CrossRef Medline

Marik SA, Yamahachi H, McManus JN, Szabo G, Gilbert CD (2010) Axonal dynamics of excitatory and inhibitory neurons in somatosensory cortex. PLoS Biol 8:e1000395. CrossRef Medline

Massie A, Cnops L, Smolders I, Van Damme K, Vandenbussche E, Vandesande F, Eysel UT, Arckens L (2003) Extracellular GABA concentrations in area 17 of cat visual cortex during topographic map reorganization following binocular central retinal lesioning. Brain Res 976:100–108. CrossRef Medline

Mataga N, Mizuguchi Y, Hensch TK (2004) Experience-dependent pruning of dendritic spines in visual cortex by tissue plasminogen activator. Neuron 44:1031–1041. CrossRef Medline

Merzenich MM, Kaas JH, Wall JT, Sur M, Nelson RJ, Felleman DJ (1983a) Progression of change following median nerve section in the cortical representation of the hand in areas 3b and 1 in adult owl and squirrel monkeys. Neuroscience 10:639–665. CrossRef Medline

Merzenich MM, Kaas JH, Wall J, Nelson RJ, Sur M, Felleman D (1983b) Topographic reorganization of somatosensory cortical areas 3b and 1 in adult monkeys following restricted deafferentation. Neuroscience 8:33–55. CrossRef Medline

Merzenich MM, Nelson RJ, Stryker MP, Cynader MS, Schoppmann A, Zook JM (1984) Somatosensory cortical map changes following digit amputation in adult monkeys. J Comp Neurol 224:591–605. CrossRef Medline

Nudo RJ, Milliken GW, Jenkins WM, Merzenich MM (1996) Use-dependent alterations of movement representations in primary motor cortex of adult squirrel monkeys. J Neurosci 16:785–807. Medline

Ozeki H, Finn IM, Schaffer ES, Miller KD, Ferster D (2009) Inhibitory stabilization of the cortical network underlies visual surround suppression. Neuron 62:578–592. CrossRef Medline

Palagina G, Eysel UT, Jancke D (2009) Strengthening of lateral activation in adult rat visual cortex after retinal lesions captured with voltage-sensitive dye imaging in vivo. Proc Natl Acad Sci U S A 106:8743–8747. CrossRef Medline

Pons TP, Garraghty PE, Ommaya AK, Kaas JH, Taub E, Mishkin M (1991) Massive cortical reorganization after sensory deafferentation in adult macaques. Science 252:1857–1860. CrossRef Medline

Priebe NJ, Ferster D (2005) Direction selectivity of excitation and inhibition in simple cells of the cat primary visual cortex. Neuron 45:133–145. CrossRef Medline

Priebe NJ, Ferster D (2006) Mechanisms underlying cross-orientation suppression in cat visual cortex. Nat Neurosci 9:552–561. CrossRef Medline

Ramachandran VS, Gregory RL (1991) Perceptual filling in of artificially induced scotomas in human vision. Nature 350:699–702. CrossRef Medline

Recanzone GH, Schreiner CE, Merzenich MM (1993) Plasticity in the frequency representation of primary auditory cortex following discrimination training in adult owl monkeys. J Neurosci 13:87–103. Medline

Robertson D, Irvine DR (1989) Plasticity of frequency organization in auditory cortex of guinea pigs with partial unilateral deafness. J Comp Neurol 282:456–471. CrossRef Medline

Rose JE, Malis LI, Kruger L, Baker CP (1960) Effects of heavy, ionizing, monoenergetic particles on the cerebral cortex. II. Histological appearance of laminar lesions and growth of nerve fibers after laminar destructions. J Comp Neurol 115:243–255. CrossRef Medline

Rosier AM, Arckens L, Demeulemeester H, Orban GA, Eysel UT, Wu YJ, Vandesande F (1995) Effect of sensory deafferentation on immunoreactivity of GABAergic cells and on GABA receptors in the adult cat visual cortex. J Comp Neurol 359:476–489. CrossRef Medline

Sanes JN, Suner S, Lando JF, Donoghue JP (1988) Rapid reorganization of adult rat motor cortex somatic representation patterns after motor nerve injury. Proc Natl Acad Sci U S A 85:2003–2007. CrossRef Medline

Sanes JN, Suner S, Donoghue JP (1990) Dynamic organization of primary motor cortex output to target muscles in adult rats. I. Long-term patterns of reorganization following motor or mixed peripheral nerve lesions. Exp Brain Res 79:479–491. Medline

Schmid LM, Rosa MG, Calford MB, Ambler JS (1996) Visuotopic reorganization in the primary visual cortex of adult cats following monocular and binocular retinal lesions. Cereb Cortex 6:388–405. CrossRef Medline

Seress L, Nitsch R, Leranth C (1993) Calretinin immunoreactivity in the monkey hippocampal formation—I. Light and electron microscopic characteristics and co-localization with other calcium-binding proteins. Neuroscience 55:775–796. CrossRef Medline

Simons DJ, Land PW (1987) Early experience of tactile stimulation influences organization of somatic sensory cortex. Nature 326:694–697. CrossRef Medline

Smirnakis SM, Brewer AA, Schmid MC, Tolias AS, Schüz A, Augath M, Inhoffen W, Wandell BA, Logothetis NK (2005) Lack of long-term cortical reorganization after macaque retinal lesions. Nature 435:300–307. CrossRef Medline

Stettler DD, Yamahachi H, Li W, Denk W, Gilbert CD (2006) Axons and synaptic boutons are highly dynamic in adult visual cortex. Neuron 49:877–887. CrossRef Medline

Sugiyama S, Di Nardo AA, Aizawa S, Matsuo I, Volovitch M, Prochiantz A, Hensch TK (2008) Experience-dependent transfer of Otx2 homeoprotein into the visual cortex activates postnatal plasticity. Cell 134:508–520. CrossRef Medline

Tan AY, Zhang LI, Merzenich MM, Schreiner CE (2004) Tone-evoked excitatory and inhibitory synaptic conductances of primary auditory cortex neurons. J Neurophysiol 92:630–643. CrossRef Medline

Trachtenberg JT, Chen BE, Knott GW, Feng G, Sanes JR, Welker E, Svoboda K (2002) Long-term in vivo imaging of experience-dependent synaptic plasticity in adult cortex. Nature 420:788–794. CrossRef Medline

Troyer TW, Krukowski AE, Priebe NJ, Miller KD (1998) Contrast-invariant orientation tuning in cat visual cortex: thalamocortical input tuning and correlation-based intracortical connectivity. J Neurosci 18:5908–5927. Medline

van Versendaal D, Rajendran R, Saiepour MH, Klooster J, Smit-Rigter L, Sommeijer JP, De Zeeuw CI, Hofer SB, Heimel JA, Levelt CN (2012) Elimination of inhibitory synapses is a major component of adult ocular dominance plasticity. Neuron 74:374–383. CrossRef Medline

van Vreeswijk C, Sompolinsky H (1998) Chaotic balanced state in a model of cortical circuits. Neural Comput 10:1321–1371. CrossRef Medline

Wallace H, Fox K (1999) The effect of vibrissa deprivation pattern on the form of plasticity induced in rat barrel cortex. Somatosens Mot Res 16:122–138. CrossRef Medline

Wehr M, Zador AM (2003) Balanced inhibition underlies tuning and sharpens spike timing in auditory cortex. Nature 426:442–446. CrossRef Medline

Weinberger NM, Javid R, Lepan B (1993) Long-term retention of learning-induced receptive-field plasticity in the auditory cortex. Proc Natl Acad Sci U S A 90:2394–2398. CrossRef Medline

Wilbrecht L, Holtmaat A, Wright N, Fox K, Svoboda K (2010) Structural plasticity underlies experience-dependent functional plasticity of cortical circuits. J Neurosci 30:4927–4932. CrossRef Medline

Xu T, Yu X, Perlik AJ, Tobin WF, Zweig JA, Tennant K, Jones T, Zuo Y (2009) Rapid formation and selective stabilization of synapses for enduring motor memories. Nature 462:915–919. CrossRef Medline

Yamahachi H, Marik SA, McManus JN, Denk W, Gilbert CD (2009) Rapid axonal sprouting and pruning accompany functional reorganization in primary visual cortex. Neuron 64:719–729. CrossRef Medline

Yang G, Pan F, Gan WB (2009) Stably maintained dendritic spines are associated with lifelong memories. Nature 462:920–924. CrossRef Medline